The solution structure of the N-terminal domain of hepatocyte growth factor reveals a potential heparin-binding site

Hongjun Zhou[1], Marie J Mazzulla[1], Joshua D Kaufman[2], Stephen J Stahl[2], Paul T Wingfield[2], Jeffrey S Rubin[3], Donald P Bottaro[3] and R Andrew Byrd[1]*

Background: Hepatocyte growth factor (HGF) is a multipotent growth factor that transduces a wide range of biological signals, including mitogenesis, motogenesis, and morphogenesis. The N-terminal (N) domain of HGF, containing a hairpin-loop region, is important for receptor binding and the potent biological activities of HGF. The N domain is also the primary binding site for heparin or heparan sulfate, which enhances receptor/ligand oligomerization and modulates receptor-dependent mitogenesis. The rational design of artificial modulators of HGF signaling requires a detailed understanding of the structures of HGF and its receptor, as well as the role of heparin proteoglycan; this study represents the first step towards that goal.

Results: We report here a high-resolution solution structure of the N domain of HGF. This first structure of HGF reveals a novel folding topology with a distinct pattern of charge distribution and indicates a possible heparin-binding site.

Conclusions: The hairpin-loop region of the N domain plays a major role in stabilizing the structure and contributes to a putative heparin-binding site, which explains why it is required for biological functions. These results suggest several basic and/or polar residues that may be important for use in further mutational studies of heparin binding.

Addresses: [1]Macromolecular NMR Section, ABL-Basic Research Program, NCI-Frederick Cancer Research and Development Center, Frederick, Maryland 21702-1201, USA, [2]Protein Expression Laboratory, National Institute of Arthritis and Musculoskeletal and Skin Diseases, National Institutes of Health, Bethesda, Maryland 20892-2775, USA and [3]Laboratory of Cellular and Molecular Biology, Division of Basic Science, National Cancer Institute, Bethesda, Maryland 20892-4255, USA.

*Corresponding author.
E-mail: rabyrd@ncifcrf.gov

Key words: hairpin loop, heparin binding, hepatocyte growth factor (HGF), NMR

Received: **19 November 1997**
Revisions requested: **15 December 1997**
Revisions received: **23 December 1997**
Accepted: **23 December 1997**

Structure 15 January 1998, **6**:109–116
http://biomednet.com/elecref/0969212600600109

Introduction

Hepatocyte growth factor (HGF) [1,2] is the prototype of a family of growth factors that resemble the blood proteinase plasminogen in sequence, domain organization, and mechanism of activation. As a mitogen, motogen, and morphogen, HGF mediates crucial aspects of development, maintenance, and regeneration of a wide variety of tissues and organs by inducing growth, movement, and differentiation of target cells. HGF is also implicated in the growth, invasion, and metastasis of tumor cells (for reviews see [3–6]). Mature HGF is composed of a 69 kDa α chain and a 34 kDa β chain. The α chain contains a well defined N-terminal domain (N; residues 31–127) followed by four 'kringle' domains (K1–K4). The β chain resembles a serine protease in sequence, but has no protease activity.

The biological activities of HGF are mediated by its receptor, c-Met, a proto-oncogene product with an intracellular tyrosine kinase domain [7–9]. Two naturally occurring, truncated HGF isoforms, NK1 (extending through K1) and NK2 (extending through K2), also bind c-Met and retain some degree of motogenic activity but differ in their abilities to stimulate DNA synthesis [10,11]. The receptor-binding determinants of HGF seem to reside primarily in the N and K1 domains. HGF also binds to heparin or heparan sulfate present on the cell surface or in the extracellular matrix. These glycosaminoglycans were found to promote ligand dimerization and enhance the proliferative activity of HGF or its variants NK1 and NK2 [12–14]. Furthermore, HGF isoforms are unable to bind c-Met in a heparan sulfate deficient cell; however, the activity was restored by addition of heparin, suggesting that heparin-like molecules may be required in the activation of c-Met [14].

The N domain of HGF plays an essential role in interactions with the c-Met receptor and heparin. This domain contains a hairpin-loop region (residues 70–96), characterized by two disulfide bonds; deletion of this region abolishes both the c-Met and heparin-binding abilities of HGF [15–17]. Similar hairpin loop regions are found in other proteins, including plasminogen and macrophage-stimulating protein [18]; activation of plasminogen results in deletion of this region. Early studies suggested that, in addition to the N domain, K2 may participate in HGF–heparin interactions [18]. More recently, however, the N domain expressed alone was shown to retain the heparin-binding properties of full-length HGF [14].

To date there is no experimental structural data for HGF or its domains. The structures of the kringle and serine

protease domains of HGF have been modeled based on sequence homology with proteins of known structures [16,19,20]. The hairpin-loop region has also been modeled, primarily using disulfide constraints [20], as there is no structural data available for the hairpin loop containing domains of plasminogen-related proteins. Because of the important roles that the hairpin-loop region plays in c-Met and heparin binding, our initial studies on HGF have focused on the N domain.

Here we report the first structural information for HGF, in the form of the solution structure of the N domain. The structure shows a novel folding motif and a major role for the hairpin-loop region in organizing and stabilizing the fold. The calculated surface positive charge distribution reveals a distinct area with high electrostatic potential, indicating a possible heparin-binding site. Correlations of our data with previous mutational studies are discussed.

Results

The recombinant N domain appears to fold in the same fashion as that found in full-length HGF. Weighted average circular dichroism (CD) spectra of the N domain and the first kringle (K1) domain match perfectly the spectrum of biologically active, recombinant NK1 [21]. Furthermore, ^{1}H and ^{15}N NMR chemical shifts for the residues in the N domain exhibit a close similarity between the spectra of N and NK1 (data not shown).

The N domain exhibits good chemical shift dispersion as evidenced in a ^{1}H-^{15}N correlation spectrum (Figure 1). Backbone NH resonance assignments were made for all residues except for the three prolines, Gly31–Asn37, Asn77 and Gly79. A weak and broadened peak was tentatively assigned to the amide of Lys78. The lack of NH resonances in the N-terminal region and residues 77–79 suggest that these regions are involved in intermediate conformational exchange. Sidechain carbon, proton, and nitrogen assignments for other regions are nearly complete. Structure calculations were based on approximately 2000 distance restraints obtained from several NOESY (nuclear Overhauser effect spectroscopy) spectra, as well as hydrogen bonds and measured torsion angles (for details see Materials and methods section).

Structure description

The overall structure of the N domain is well defined (Figure 2; Table 1) except for Asn77–Gly79 and the N-terminal seven residues in which NMR data were not observed or the resonance assignments were tentative. The middle of the structure is a five-stranded antiparallel β sheet formed by residues 42–46 (β1), 60–63 (β2), 86–90 (β3), 95–99 (β4), and 117–121 (β5), arranged in the spatial order β1–β5–β3–β4–β2 (Figure 3). The β sheet is flanked on one side by a two-turn α helix (residues 67–75), a short 3_{10} helix (residues 39–41), and the N-terminal residues; on the other side it is flanked by two extended loops (residues 47–59 and 100–116) joining the opposite ends of the β strands. This organization makes a three-layered sandwich structure. NOE patterns between residues 49–51 and residues 109–111, along with their Cα and CO carbon chemical shift indices [22] and $^{3}J_{HNH\alpha}$ coupling constants [23], indicate that these regions form a sheet-like structure. A hydrophobic core is formed primarily by nonpolar residues in strand β5 and the β-hairpin structure formed by β3 and β4. Backbone amides in these three strands are strongly protected from hydrogen exchange with solvent. The two extended loops run across the back of the central β sheet, shielding the core residues from solvent.

Figure 1

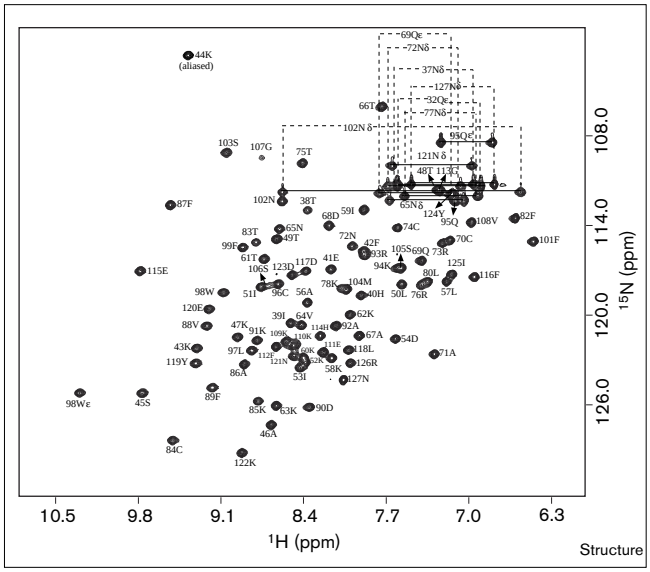

Two-dimensional ^{1}H-^{15}N correlation spectrum of the N domain of HGF, labeled with assignments of backbone amides and sidechain NH_2 groups.

Structure of the hairpin-loop region

The hairpin-loop region is composed of the α helix and strands β3 and β4 in the central β sheet (Figure 4). The inner Cys74–Cys84 disulfide linkage connects the C terminus of the α helix and the N terminus of strand β3, generally resembling the fold that was previously modeled based on disulfide restraints [20]. The outer Cys70–Cys96 disulfide linkage connects the middle of the helix and the middle of strand β4. The hairpin-loop region has a fold of the type α–loop–β–loop–β, but not α–loop–β–loop–α as previously suggested [20]. The α–loop–β–loop–β structure exposes Arg93 on a surface separate from the surface containing Arg73 and Arg76, which is different from the modeled structure. The four cysteines participate in favorable interactions with several aromatic rings, including those of Phe87 and Trp98. The interacting sulfur atoms

Figure 2

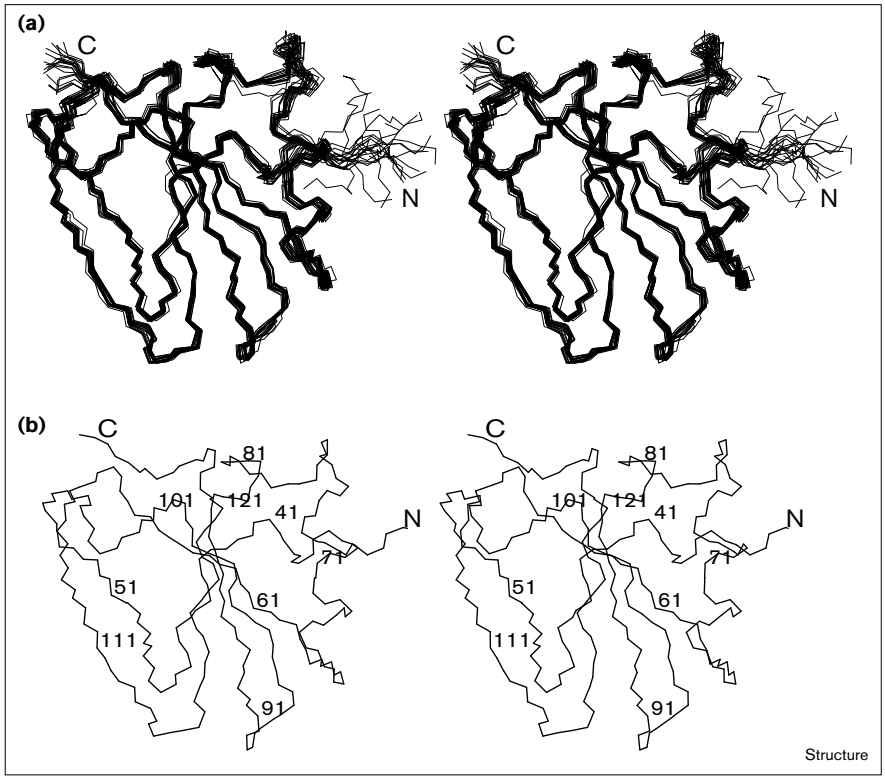

Stereo diagram of the N domain of HGF. **(a)** Superposition of the backbone heavy atoms (N, Cα and C′) of 20 NMR structures for the N domain of HGF. **(b)** Backbone diagram of the restrained minimized average structure with every tenth residue labeled.

express an affinity towards the edge of the aromatic rings, as has been found in many other proteins [24]. The backbone structure of the hairpin-loop region, except for Arg76–Gly79, is fairly rigid, indicated by the small deviations between the 20 NMR structures (Figure 2). Residues 77–79 reside in the loop joining the α helix and strand β3. This region is likely to be involved in intermediate conformational exchange, suggested by the absence or broadening of amide cross-peaks.

Identification of a possible heparin-binding site

Studies of several heparin-binding proteins suggest that binding occurs between specific domains of clustered basic amino acids and the sulfate and carboxylate groups of heparin [25]. The N domain contains 23 lysine and arginine residues, seven of which are located in the hairpin-loop region, and it is reasonable to suggest that some spatial clusters of these residues are involved in heparin binding.

A comparison of the heparin-binding site of basic fibroblast growth factor (bFGF) with the structure of the N domain reveals distinct patterns of basic charge distribution. The surface of bFGF bound to heparin [26] has high positive electrostatic potential (Figure 5a), where heparin binding is stabilized by charge interactions with lysine and arginine residues, as well as hydrogen bonds with asparagine and glutamine sidechains. In the N domain, an

Table 1

Structural statistics and root mean square deviations for 20 NMR structures of the N domain of HGF.

Structural statistics*	<SA>	$\langle SA \rangle_r$
Rmsd from experimental distance (Å) and dihedral angle (°) restraints†		
all (1977)	0.013 ± 0.007	0.010
interresidue |i–j| >4 (633)	0.008 ± 0.001	0.007
interresidue 1 ≤|i–j|≤4 (620)	0.009 ± 0.001	0.009
intraresidue (724)	0.014 ± 0.002	0.014
hydrogen bonds (20)	0.013 ± 0.007	0.010
dihedral ϕ (37)	0.74 ± 0.18	0.60
Rmsd from idealized geometry used within X-PLOR		
bonds (Å)	0.0037 ± 0.0001	
angles (°)	0.65 ± 0.01	
impropers (°)	0.48 ± 0.18	
Cartesian coordinates rmsd‡		
$\langle SA \rangle$ versus <SA> all	0.37 ± 0.007§	0.91 ± 0.09#

*<SA> are the 20 NMR-derived structures. $\langle SA \rangle$ is the mean structure obtained by averaging the coordinates of the 20 structures. $\langle SA \rangle_r$ is the restrained minimized average structure. For <SA>, the rmsd is the average rmsd and the standard deviations for the 20 structures. †None of the structures have distance violations ≥ 0.5 Å or dihedral angle violations ≥ 5°. ‡The rmsd between the 20 structures and the mean coordinates for residues 40–124. §Values for backbone atoms; #values for all nonhydrogen atoms.

Figure 3

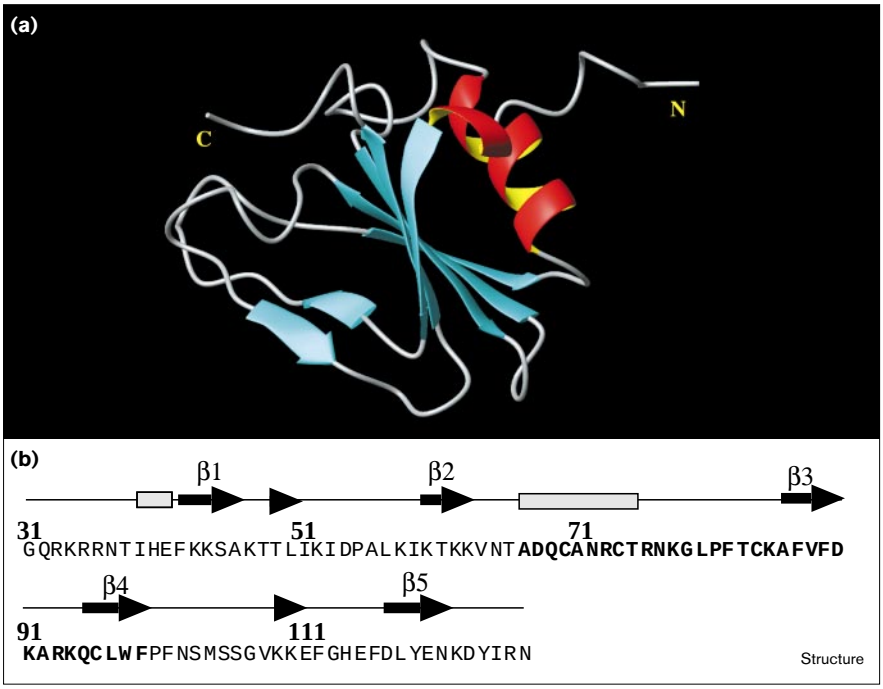

Solution structure and secondary structure alignment. **(a)** Ribbon plot depicting the structure of the N domain of HGF. The structure was generated by averaging 20 NMR structures followed by restrained minimization. Helices are shown in red and yellow, β strands are in blue. **(b)** Sequence and secondary structure of the N domain; the numbering scheme follows that in [21]. The hairpin-loop sequence, highlighted in bold letters, extends from Ala67 to Phe99 based on the structure. The β strands are indicated by arrows and the helices by rectangles. (Ribbon plot was generated with the program MOLMOL [41].)

area containing basic residues in strand β2 and basic and polar residues in the α helix of the hairpin loop also has high positive potential (Figure 5b). This distinct area, which may serve as a heparin-binding site, includes Lys60, Lys62, Arg73, Arg76, and Lys78 (Figure 6a). These residues form an arch of positive charges on the surface, with Lys60, Lys62, and Arg73 at the center. This region also contains the highest density of asparagine and glutamine residues, which are clustered on one side of the α helix near the high positive potential area. Although there is some degree of uncertainty in sidechain orientation due to intrinsic flexibility (e.g. residues 76 and 78) or because of the lack of distance restraints in the unbound form of the protein, this does not seem to change the clustering of positive charges in this region (Figure 6b).

Figure 4

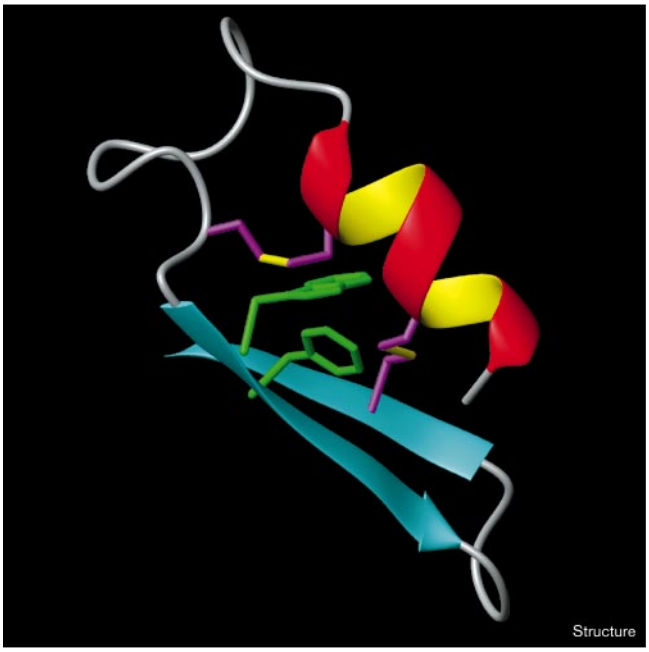

Structure of the hairpin-loop region. Secondary structure elements are colored as described in Figure 3a; the two disulfide bonds are shown in yellow. Also shown (in green) are Phe87 and Trp98 with their rings interacting with sulfur atoms.

Discussion

Role of the hairpin loop

The hairpin-loop region consists of an α helix followed by a β-hairpin structure. Given the constraints imposed by the two disulfide bridges, it is reasonable to believe that the α–loop–β–loop–β motif is shared by the hairpin-loop regions of other plasminogen-related proteins. The hairpin-loop region plays a major role in organizing the protein scaffold and in contributing a number of residues, including several aromatic residues, to the hydrophobic core. In addition to its role in stabilizing the fold, this region also forms part of the putative heparin-binding site. The marked decrease in heparin- and receptor-binding affinities of HGF after deletion of the hairpin loop [17,18] is likely to be due to the loss of a binding epitope in the native structure of the N domain. It is

Figure 5

Front and back views of the surface electrostatic potential maps of **(a)** bFGF and **(b)** the N domain of HGF. The positive potential area is shown in blue; the negative potential is in red. Arrows indicate the heparin-binding site of bFGF and the potential heparin-binding site of the N domain of HGF. (Figures were generated with the program GRASP [42].)

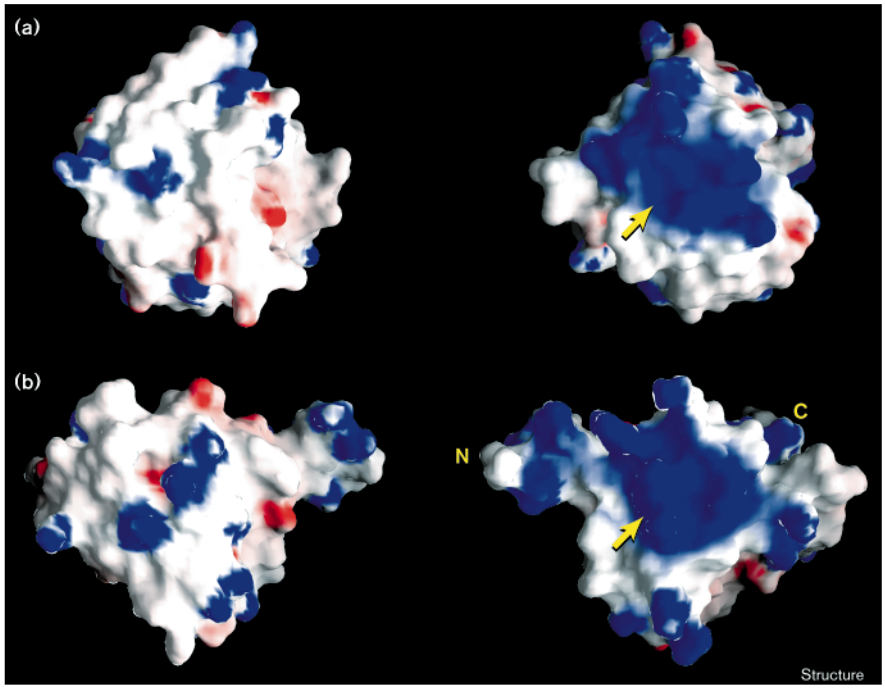

possible that a fragment of this domain containing the hairpin-loop region is able to retain some elements of the native fold, especially in the presence of heparin which may stabilize the fold. Indeed, a proteolytic peptide fragment, Phe42–Glu111, exhibits a transition from a random structure to a β sheet like structure upon high-affinity binding to heparin, as shown by CD spectra [27].

Correlations with heparin-binding studies

Several biochemical studies of heparin-binding have yielded inconclusive results concerning which residues are involved in binding. A correlation between the net charge of the hairpin loop and the heparin-binding abilities of HGF and closely related proteins has been noted. In addition, a proteolytic peptide fragment of HGF, Asp68–Glu111, has been shown to bind heparin with high affinity [27]. Based on the N domain structure, however, it is not clear that this peptide would retain native folding without the flanking strands of the central β sheet. Furthermore, alanine substitutions of several basic residues in this region caused only small reductions in heparin binding [14]. These data suggest that the basic and polar residues in

Figure 6

Residues that may have biological significance. **(a)** The basic residues that form the potential heparin-binding site indicated in Figure 5b are shown in red. Yellow spheres indicate the two basic residue clusters in the hairpin-loop region that have been subjected to alanine-substitution studies of heparin binding [14]. Green spheres indicate the residues that either reduce receptor binding or the biological activities of the HGF variant NK1 upon alanine substitution [16]. **(b)** Overlay of 20 NMR structures of the putative heparin-binding site, showing the dispersion in sidechain orientations of the basic residues (shown in red). The structure is slightly rotated relative to (a) for more clarity. (The backbone trace diagram was generated with the program RASMOL [43].)

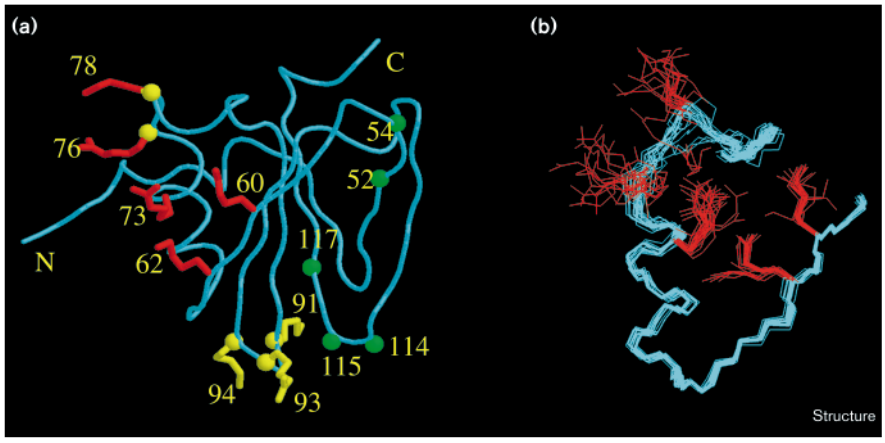

the hairpin loop which are not clustered (e.g. Asn72 and Arg73), as well as residues outside the hairpin loop (e.g. Lys60 and Lys62), may contribute to heparin binding. This view is supported by the structural data presented here.

Compared to bFGF, the N domain exhibits a wider distribution of basic residues over its surface, although there is a single, predominant positive potential area. The two basic residue clusters in the hairpin-loop region (Lys91, Arg93, Lys94 and Arg76, Lys78) reside in the turn or loop regions, outside or at the edge of the putative heparin-binding site (Figure 6). Their positions are consistent with the small effects on heparin-binding upon alanine substitution of these residues. The critical residues involved in heparin-binding are possibly Arg73, Lys60, and Lys62. Other adjacent basic residues, including the highly positively charged N-terminal region and two other positive charge clusters (Lys52, Lys58 and Lys63, Lys91, Arg93, Lys94), may contribute additively to binding, depending on the length and composition of the heparin or heparin-like molecules. These findings are consistent with the larger size of the heparin-derived oligosaccharide required for high-affinity binding to HGF (12–14 residues) versus bFGF (5 residues) [28]. It is not clear, however, if some of these basic residue clusters are excluded from interactions with heparin by the kringle domain(s) in full-length HGF or in a multidomain fragment. Nevertheless, there does not appear to be extensive contacts between the N and K1 domains, and the high surface potential area is located on a different side of the N domain structure from the C terminus, making it unlikely to be occluded by K1. NMR-monitored titration experiments may help to further delineate the heparin-binding site(s).

The overall topology of the N domain is unusual among known protein structures, and is characterized by the two extended loops joining the opposite ends of the central β sheet. A search of the protein data bank (PDB) using the program DALI [29] failed to find a similar folding pattern among known protein structures. It is interesting to note that alanine substitutions of several residues at or near the turn regions joining the extended loops and the central β sheet caused a significant reduction in the mitogenic and/or receptor-binding abilities of the HGF variant NK1 (Figure 6a) [16]. These results suggest that the loop regions may have important roles in receptor binding and/or stabilization of the fold.

Biological implications

Hepatocyte growth factor (HGF) is a potent mitogen, motogen, and morphogen, which targets a wide range of tissues and organs, and is also implicated in tumorigenesis. HGF exerts its effects through a receptor tyrosine kinase, but also binds heparin which profoundly effects its biological activities. HGF is one of the few known plasminogen-related growth factors, each having an N-terminal (N) domain with a hairpin-loop sequence. While this domain becomes truncated when plasminogen is converted to its active form, it is retained in mature HGF and is essential for the HGF–receptor and HGF–heparin interactions.

The HGF N domain structure reported here, represents the first structure of this domain from any plasminogen-related protein. The structure reveals a distinct pattern of positive charge distribution, and an unusual folding topology which may be unique to this class of proteins. The hairpin-loop region, folded in a well defined α–loop–β–loop–β motif, not only plays an important role in stabilizing the structure, but also contributes several basic residues to a putative heparin-binding site. In light of the N domain structure, and prior reports that basic residues outside or at the edge of this site have little effect on heparin binding, we propose that three basic residues together with several polar residues may play critical roles in heparin binding.

The high intrinsic stability of the N domain structure, when expressed without the adjoining domains of HGF, suggests that it, like the kringle and serine protease domains, may have been incorporated into the relatively complex HGF domain structure by genetic recombination events involving a gene(s) encoding a simpler ancestral protein. The extent to which this structure is distributed among existing proteins, and whether it occurs independently of other structural domains, will help elucidate the origins of this unique class of signaling molecules.

Materials and methods

NMR sample preparation

Both ^{15}N- and $^{15}N/^{13}C$-labeled forms of the N domain of HGF were produced in *Escherichia coli* and purified as described previously [21] except that M9 minimal media, containing either $^{15}NH_4Cl$ or both $^{15}NH_4Cl$ and ^{13}C-labeled glucose, was used during the protein expression. The final NMR sample conditions were: 50 mM $NaPO_4$, 100 mM NaCl, 0.02% sodium azide, pH 6.8, at a concentration of ~2 mM, in either 8% D_2O/92% H_2O or 100% D_2O.

Data collection and analysis

All NMR data were collected on a Varian UnityPlus 600 MHz spectrometer at 30°C using Z-spec triple resonance probes with pulsed field gradients (Nalorac Corp., Martinez, CA). Sequential connectivities of the NH spin systems were established in three-dimensional (3D) HNCACB and CBCACONNH experiments [30]. Residue type identification and sidechain $^1H/^{13}C$ resonance assignments were made using 3D HCCONH and CCONH experiments [31]. Two-dimensional (2D) HBCBCGCDHD and HBCBCGCDCEHE experiments [32], along with observed intraresidue NOEs, were used to assign aromatic ring proton and carbon resonances. Distance restraints were determined from 3D ^{15}N-edited NOESY [33], four-dimensional (4D) $^{15}N/^{13}C$-edited NOESY [34], and 4D $^{13}C/^{13}C$-edited NOESY [35] with a mixing time of 150 ms. Coupling constants between NH protons and CαH protons ($^3J_{HNH\alpha}$) were measured as described [36]. Four high-resolution, 2D ^1H-^1H NOESY [37] and ^1H-^1H correlation spectroscopy (COSY) [38] spectra collected from samples in H_2O or D_2O were used to aid resonance assignments.

Structure calculations

Structure calculations were performed using the program X-PLOR [39] and the distance-geometry simulated-annealing (SA) methods [40]. The NOEs were classified according to their integrated volume in three distance ranges: strong, 1.8–3.0 Å; medium: 1.8–3.8 Å and weak, 1.8–5.0 Å. The locations of the two disulfide bonds were confirmed by initial calculations using only NOE restraints; subsequent calculations included specific disulfide bond restraints. Dihedral angle and hydrogen-bond restraints were applied at the final stage of refinement. The dihedral angles ϕ were estimated from $^3J_{HNH\alpha}$ and were used to restrain the helix or strand regions as $-60 \pm 40°$ for $^3J_{HNH\alpha} < 6$ Hz and $-120 \pm 40°$ for $^3J_{HNH\alpha} > 8$ Hz [23]. Hydrogen-bond restraints were included based on cross-strand NOE patterns for the sheet region or for those slowly exchanging amides in a helix or strand identified in a ^1H-^{15}N correlation spectrum following solvent exchange with D_2O. Each hydrogen bond was applied with two distance restraints, one between the hydrogen and acceptor atom of 1.5–2.3 Å and one between the donor heavy atom and the acceptor atom of 2.4–3.3 Å. Twenty low-energy NMR structures were selected and final structures were obtained by 2500 steps of Powell minimization. The energy terms included in the calculation and their final force constant values are: bonds, 1000 kcal mol^{-1} Å^{-2}; van der Waals repel force, 4 kcal mol^{-1} Å^{-4}, with a repel radii of 0.75 of those in the X-PLOR parameter set; angles, 500 kcal mol^{-1} rad^{-2}; improper angles as defined in the X-PLOR 3.8 parameter file (parallhdg.pro); dihedral, 200 kcal mol^{-1} rad^{-2}; and NOE, 50 kcal mol^{-1} Å^{-2}.

Accession numbers

The coordinates have been deposited in the Brookhaven protein data bank with accession code 2hgf.

Acknowledgements

We thank Lewis K Pannell (National Institute of Diabetes and Digestive and Kidney Diseases, NIDDK, National Institutes of Health, NIH) for assistance with mass spectrometry. This research was sponsored in part by the National Cancer Institute, Department of Health and Human Services (DHHS) under contract with ABL. The contents of this publication do not necessarily reflect the views or policies of the Department of Health and Human Services, nor does mention of trade names, commercial products, or organizations imply endorsement by the US Government.

References

1. Miyazawa, K., *et al*., & Takahashi, K. (1989). Molecular cloning and sequence analysis of cDNA for human hepatocyte growth factor. Biochem. Biophys. Res. Commun. 163, 967–973.
2. Nakamura, T., *et al*., & Shimizu, S. (1989). Molecular cloning and expression of human hepatocyte growth factor. *Nature* **342**, 440–443.
3. Matsumoto, K. & Nakamura, T. (1996). Emerging multipotent aspects of hepatocyte growth factor. *J. Biochem.* **119**, 591–600.
4. Rosen, E.M., Nigam, S.K. & Goldberg, I.D. (1994). Scatter factor and the c-met receptor: a paradigm for mesenchymal/epithelial interaction. *J. Cell Biol.* **127**, 1783–1787.
5. Zarnegar, R. & Michalopoulos, G.K. (1995). The many faces of hepatocyte growth factor: from hepatopoiesis to hematopoiesis. *J. Cell Biol.* **129**, 1177–1180.
6. Rubin, J.S., Bottaro, D.P. & Aaronson, S.A. (1993). Hepatocyte growth factor/scatter factor and its receptor, the c-met proto-oncogene product. *Biochem. Biophys. Acta* **1155**, 357–371.
7. Bottaro, D.P., *et al*., & Aaronson, S.A. (1991). Identification of the hepatocyte growth factor receptor as the c-met proto-oncogene product. *Science* **251**, 802–804.
8. Naldini, L., Vigna, E., Narsimhan, R., Gaudino, G., Zarnegar, R., Michalopoulos, G.K. & Comoglio, P.M. (1991). Hepatocyte growth factor (HGF) stimulates the tyrosine kinase activity of the receptor encoded by the proto-oncogene c-MET. *Oncogene* **6**, 501–504.
9. Higuchi, O., Mizuno, K., Vande Woude, G.F. & Nakamura, T. (1992). Expression of c-met proto-oncogene in COS cells induces the signal transducing high-affinity receptor for hepatocyte growth factor. *FEBS Lett.* **301**, 282–286.
10. Cioce, V., *et al*., & Rubin, J.S. (1996). Hepatocyte growth factor (HGF)/NK1 is a naturally occurring HGF/scatter factor variant with partial agonist/antagonist activity. *J. Biol. Chem.* **271**, 13110–13115.
11. Chan, A.M., Rubin, J.S., Bottaro, D.P., Hirschfield, D.W., Chedid, M. & Aaronson, S.A. (1991). Identification of a competitive HGF antagonist encoded by an alternative transcript. *Science* **254**, 1382–1385.
12. Zioncheck, T.F., *et al*., & Stack, R.J. (1995). Sulfated oligosaccharides promote hepatocyte growth factor association and govern its mitogenic activity. *J. Biol. Chem.* **270**, 16871–16878.
13. Schwall, R.H., *et al*., & Zioncheck, T.F. (1996). Heparin induces dimerization and confers proliferative activity onto the hepatocyte growth factor antagonists NK1 and NK2. *J. Cell Biol.* **133**, 709–718.
14. Sakata, H., *et al*., & Rubin, J.S. (1997). Heparin binding and oligomerization of hepatocyte growth factor/scatter factor isoforms. Heparan sulfate glycosaminoglycan requirement for Met binding and signaling. *J. Biol. Chem.* **272**, 9457–9463.
15. Matsumoto, K., Takehara, T., Inoue, H., Hagiya, M., Shimizu, S. & Nakamura, T. (1991). Deletion of kringle domains or the N-terminal hairpin structure in hepatocyte growth factor results in marked decreases in related biological activities. *Biochem. Biophys. Res. Commun.* **181**, 691–699.
16. Lokker, N.A., Presta, L.G. & Godowski, P.J. (1994). Mutational analysis and molecular modeling of the N-terminal kringle-containing domain of hepatocyte growth factor identifies amino acid side chains important for interaction with the c-Met receptor. *Protein Eng.* **7**, 895–903.
17. Okigaki, M., Komada, M., Uehara, Y., Miyazawa, K. & Kitamura, N. (1992). Functional characterization of human hepatocyte growth factor mutants obtained by deletion of structural domains. *Biochemistry* **31**, 9555–9561.
18. Mizuno K., *et al*., & Nakamura, T. (1994). Hairpin loop and second kringle domain are essential sites for heparin binding and biological activity of hepatocyte growth factor. *J. Biol. Chem.* **269**, 1131–1136.
19. Lokker, N.A., *et al*., & Godowski, P.J. (1992). Structure-function analysis of hepatocyte growth factor: identification of variants that lack mitogenic activity yet retain high affinity receptor binding. *EMBO J.* **7**, 2503–2510.
20. Donate, L.E., Gherardi, E., Srinivasan, N., Sowdhamini, R., Aparicio, S. & Blundell, T.L. (1994). Molecular evolution and domain structure of plasminogen-related growth factors (HGF/SF and HGF1/MSP). *Protein Sci.* **3**, 2378–2394.
21. Stahl, S.J., *et al*., & Bottaro, D.P. (1997). Functional and biophysical characterization of recombinant human hepatocyte growth factor isoforms produced in *Escherichia coli*. *Biochem. J.* **326**, 763–772.
22. Wishart, D.S. & Sykes, B.D. (1994). The ^{13}C chemical-shift index: a simple method for the identification of protein secondary structure using ^{13}C chemical-shift data. *J. Biomol. NMR* **4**, 171–180.
23. Wüthrich, K. (1986). *NMR of Proteins and Nucleic Acids*. Wiley, New York.
24. Reid, K.S.C., Lindley, P.F. & Thornton, J.M. (1985). Sulphur–aromatic interactions in proteins. *FEBS Lett.* **190**, 209–213.
25. Jackson, R.L., Busch, S.J. & Cardin, A.D. (1991). Glycosaminoglycans: molecular properties, protein interactions, and role in physiological processes. *Physiol. Rev.* **71**, 481–539.
26. Faham, S., Hileman, R.E., Fromm, J.R., Linhardt, R.J. & Rees, D.C. (1996). Heparin structure and interactions with basic fibroblast growth factor. *Science* **271**, 1116–1120.
27. Aoyama, H., *et al*., & Hayase, T. (1997). Isolation and conformational analysis of fragment peptide corresponding to the heparin-binding site of hepatocyte growth factor. *Biochemistry* **36**, 10286–10291.
28. Lyon, M., Deakin, J.A., Mizuno, K., Nakamura, T. & Gallagher, J.T. (1994). Interaction of hepatocyte growth factor with heparan sulfate. Elucidation of the major heparan sulfate structural determinants. *J. Biol. Chem.* **269**, 11216–11223.
29. Holm, L. & Sander, C. (1993). Protein structure comparison by alignment of distance matrices. *J. Mol. Biol.* **233**, 123–138.
30. Muhandiram, D.R. & Kay, L.E. (1994). Gradient-enhanced triple-resonance three-dimensional NMR experiments with improved sensitivity. *J. Magn. Reson. B* **103**, 203–216.
31. Grzesiek, S., Anglister, J. & Bax, A. (1993). Correlation of backbone amide and aliphatic sidechain resonances in $^{13}C/^{15}N$-enriched proteins by isotropic mixing of ^{13}C magnetization. *J. Magn. Reson. B* **101**, 114–119.
32. Yamazaki, T., Forman-Kay, J.D. & Kay, L.E. (1993). Two-dimensional NMR experiments for correlating $^{13}C^{\beta}$ and $H^{\delta}/^{\varepsilon}$ chemical shifts of aromatic residues in ^{13}C-labeled proteins via scalar couplings. *J. Am. Chem. Soc.* **115**, 11054–11055.
33. Zhang, O., Kay, L.E., Olivier, J.D. & Forman-Kay, J.D. (1994). Backbone ^1H and ^{15}N resonance assignments of the N-terminal SH3 domain of drk in folded and unfolded states using enhanced-sensitivity pulsed field gradient NMR techniques. *J. Biomol. NMR* **4**, 845–858.

34. Muhandiram, D.R., Xu, G.Y. & Kay, L.E. (1993). An enhanced-sensitivity pure absorption gradient 4D ^{15}N,^{13}C-edited NOESY experiment *J. Biomol. NMR* **3**, 463–470.
35. Vuister, G.W., *et al*., & Bax, A. (1993). Increased resolution and improved spectral quality in four-dimensional $^{13}C/^{13}C$-separated HMQC-NOESY-HMQC spectra using pulsed field gradients. *J. Magn. Reson. B* **101**, 210–213.
36. Kuboniwa, H., Grzesiek, S., Delaglio, F. & Bax, A. (1994). Measurement of HN–H alpha J couplings in calcium-free calmodulin using new 2D and 3D water-flip-back methods. *J. Biomol. NMR* **4**, 871–878.
37. Macura, S. & Ernst, R.R. (1980). Elucidation of cross relaxation in liquids by two-dimensional N.M.R. spectroscopy. *Mol. Phys.* **41**, 95–117.
38. Altieri, A.S. & Byrd, R.A. (1995). Randomization approach to water suppression in multidimensional NMR using pulsed field gradients. *J. Magn. Reson. B* **107**, 260–266.
39. Brünger, A.T. (1992). *X-PLOR 3.1: a System for X-ray Crystallography and NMR* . Yale University Press, New Haven, CT.
40. Nilges, M., Clore, G.M. & Gronenborn, A.M. (1988). Determination of three-dimensional structures of proteins from interproton distance data by dynamical simulated annealing from a random array of atoms. Circumventing problems associated with folding. *FEBS Lett.* **229**, 317–324.
41. Koradi, R., Billeter, M. & Wüthrich, K. (1996). MOLMOL: a program for display and analysis of macromolecular structures. *J. Mol. Graph.* **14**, 51–55.
42. Nicholls, A., Sharp, K. & Honig, B. (1991). Protein folding and association: insights from the interfacial and thermodynamic properties of hydrocarbons. *Proteins* **11**, 281–296.
43. Sayle, R. & Milner-White, E.J. (1995). RasMol: biomolecular graphics for all. *Trends Biochem. Sci.* **20**, 374.